Circular Folding Cooperative Power Spectral Density Split Cancellation Algorithm

Roberto C. D. V. Bomfin, Rausley A. A. de Souza, *Member, IEEE*, and Dayan A. Guimarães

***Abstract*—The cooperative power spectral density split cancellation (CPSC) algorithm for spectrum sensing has low computational complexity and is robust under dynamical noise. We propose a novel circular folding CPSC (CF-CPSC) algorithm that expressively outperforms the original CPSC. Making use of the incomplete regularized Beta function, the cumulative distribution functions of the main random variables that form the decision statistic of the CF-CPSC model are derived. It is also derived an expression for the global probability of false alarm of the CF-CPSC, which is particularized to an approximate simple closed form that yields very accurate results. A closed-form expression of the decision threshold is provided as well. The analytical results are verified by Monte Carlo simulations. Other simulation results are provided to demonstrate the suitability of the CF-CPSC for scenarios of practical interest.**

***Index Terms*—Cognitive radio, cooperative power spectral density split cancellation, spectrum sensing, dynamical noise.**

I. Introduction

THE development of new wireless communication systems will have to cope with the exponentially increasing service demand, and with the spectrum scarcity inherited by the fixed channel allocation policy adopted around the world. A potential solution is the cognitive radio (CR) concept, which allows for an efficient use of the radio resources [1]. One of the CR objectives is the dynamic access to the radio-frequency spectrum. To this end, each secondary user (SU) of the CR network has to implement the spectrum sensing function, which consists of collecting samples from the licensed user, or primary user (PU) signal in order to find vacant bands (spectral holes) for subsequent access.

Studies have shown that multipath fading and shadowing contribute to the performance degradation of the the spectrum sensing, and that cooperative spectrum sensing (CSS) schemes can combat these impairments and reduce the complexity of the CRs [1]. In the centralized data-fusion CSS, which is one of the CSS schemes, the CRs in cooperation send the collected samples of the received signal, or some information derived from these samples to a central element of the secondary network, known as fusion center (FC). The FC makes a global decision about whether the sensed bandwidth is vacant or not. Nonetheless, noise variance differences at the input of the CRs may degenerate the CSS performance; robust spectrum sensing techniques have been developed to tackle this problem, for instance the cooperative power spectral density split cancellation (CPSC) method [1], [2]. The effectiveness of the algorithm that combines data from various CRs to reach the global decision is critical, since incorrect detections affect the throughput of the SUs and may cause interference to the PUs. Consequently, designing such an algorithm is a challenge to be faced.

The CPSC method originally proposed in [1] has the main advantages of low computational complexity and robustness against dynamical noise. In this letter we propose a modified CPSC algorithm, which we call circular folding CPSC (CF-CPSC). Significant performance improvements of the CF-CPSC over the original CPSC are reported. We also derive the cumulative distribution function (CDF) of the main random variables that form the decision statistic of the CF-CPSC model, and an expression for its global probability of false alarm (PFA). This expression is then particularized to a simple approximate closed form. Monte Carlo simulations confirm the accuracy of the analytical results.

II. System Model and the CF-CPSC Algorithm

During the sensing interval, the n-th sample, $n = 1, \dots, M$, M even, of the signal received from the PU transmitter by the u-th CR, $u = 1, 2, \dots, U$, is $x_u(n) = w_u(n)$ under the $\mathcal{H}_0$ hypothesis (absence of the PU signal), or $x_u(n) = \sum_{z=0}^{Z-1} h_u(z)s(n-z) + w_u(n)$ under the $\mathcal{H}_1$ hypothesis (presence of the PU signal), with $w_u(n)$ being the circularly-symmetric additive Gaussian noise with zero mean. Under $\mathcal{H}_1$, the unknown and deterministic transmitted PU signal $s(n)$ is convolved with the unknown Z-tap channel impulse response $h_u(z)$ that represents the time-varying channel between the PU and the u-th CR, which is assumed to be fixed during the sensing interval. If $Z = 1$, $h_u(z)$ denotes a flat and slow shadowed-fading channel. If $Z > 1$, $h_u(z)$ corresponds to a frequency-selective and slow shadowed-fading channel.

A. The CF-CPSC Algorithm

The proposed CF-CPSC algorithm follows the steps:

① Compute $X_u(k)$, the discrete Fourier transform (DFT) of $x_u(n)$, $k = 1, \dots, M$.

② Compute the instantaneous power spectral density (PSD) of $x_u(n)$ as $F'_u(k) = |X_u(k)|^2/M$, and compute $F_u(k)$ as

$$F_u(k) = \begin{cases} \frac{F'_u(1)+F'_u(M/2+1)}{2}, & k = 1 \\ \frac{F'_u(k)+F'_u(M-k+2)}{2}, & k = 2, 3, \dots, M. \end{cases} \quad (1)$$

Manuscript received August 26, 2015; accepted September 21, 2015. Date of publication January 1, 2017; date of current version April 1, 2017. This work was supported by Finep (with Funttel resources) Grant 01.14.0231.00, under the Radiocommunications Reference Center (CRR) project of the National Institute of Telecommunications (Inatel), Brazil. The associate editor coordinating the review of this paper and approving it for publication was Fanggang WANG. R. C. D. V. Bomfin is with the Vodafone Chair Mobile Communication Systems, Technische Universität Dresden, Germany (e-mail: roberto.bomfin@ifn.et.tu-dresden.de). R. A. A. de Souza and D. A. Guimarães are with Inatel, Brazil (e-mail: rausley@inatel.br; dayan@inatel.br).

③ Divide $F_u(k)$ into $2L$ sub-bands, with $V = M/(2L)$ samples each. Compute $F_{\ell,u} = \sum_{k=1}^{V} F_u\left[(\ell-1)V + k\right]$, with $\ell = 1, 2, \ldots, L$ denoting the ℓ-th sub-band, and $F_{\text{full}_u} = \sum_{k=1}^{M/2} F_u(k)$, where ℓ up to L and the sum up to $M/2$ can be adopted due to the even symmetry of $F_u(k)$ about $M/2+1$.
④ To cancel the noise variance, compute, for each sub-band and each CR, $r_u(\ell) = F_{\ell,u}/F_{\text{full}_u}$, which form the test statistics that will be sent to the FC.
⑤ At the FC, average $r_u(\ell)$ over all CRs to obtain the decision variable for each sub-band, which is $r_{\text{avg}}(\ell) = \sum_{u=1}^{U} r_u(\ell)/U$.
⑥ Compare $r_{\text{avg}}(\ell)$, $\ell = 1, 2, \ldots, L$, with the threshold γ in order to decide upon each sub-band occupation: if $r_{\text{avg}}(\ell) < \gamma$, decide $\mathcal{H}_0$; decide $\mathcal{H}_1$ otherwise.
⑦ Make the final decision $\mathcal{H}_0$ if all sub-bands were decided $\mathcal{H}_0$; decide $\mathcal{H}_1$ if at least one sub-band was decided $\mathcal{H}_1$.

The fundamental difference between the original CPSC of [1] and the proposed CF-CPSC is in step ②: in the CPSC algorithm $F_u(k) = F'_u(k)$; here it is applied a modified circular-even component [3, eq. (5.33)] of $F'_u(k)$ in which $F_u(1) = F'_u(1)$ was changed to $F_u(k) = [F'_u(1) + F'_u(M/2+1)]/2$. The acronym CF-CPSC was coined due to the fact that the circular-even component of a sequence is defined based on the circular-folding operation [3, p. 169].

B. Mean and Variance of Power Spectral Densities

The mean and variance of $F_u(k)$ and $F'_u(k)$, $k > 1$, are derived in this subsection to reveal why the CF-CPSC outperforms the CPSC. Intermediate tedious derivations are omitted due to space restrictions.

Let the PU signal samples be written as $s(n) = s_{\text{I}}(n) + js_{\text{Q}}(n)$, and let $S(k)$, $S_{\text{I}}(k)$, $S_{\text{Q}}(k)$, $W_u(k)$ and $H_u(k)$ be the DFTs of $s(n)$, $s_{\text{I}}(n)$, $js_{\text{Q}}(n)$, $w_u(n)$ and $h_u(z)$, respectively. In order to confer tractability to the derivations, it is assumed a flat fading channel, i.e. $H_u(k)$ is the same for all k. Dropping the CR index u and the frequency index k for the notational simplicity, $F'_u(k)$ and (1) are written respectively as

$$F'_u(k) = F_{s_{\text{I}}} + F_{s_{\text{Q}}} + F_{s_{\text{I}}s_{\text{Q}}} + F_w^{\text{e}} + F_w^{\text{o}} + F_{sw}^{\text{e}} + F_{sw}^{\text{o}} \tag{2}$$
$$F_u(k) = F_{s_{\text{I}}} + F_{s_{\text{Q}}} + F_w^{\text{e}} + F_{sw}^{\text{e}}, \tag{3}$$

where the superscripts e and o denote circular-even and circular-odd [3, eq. (5.33)] components, respectively. $F_{s_{\text{I}}} = |H_u(k)|^2|S_{\text{I}}(k)|^2/M$, $F_{s_{\text{Q}}} = |H_u(k)|^2|S_{\text{Q}}(k)|^2/M$ and $F_w = |W(k)|^2/M = F_w^{\text{e}} + F_w^{\text{o}}$ are PSDs, with $F_{s_{\text{I}}}$ and $F_{s_{\text{Q}}}$ being circular-even sequences. Using the superscripts r and i to denote real and imaginary parts, respectively, $F_{s_{\text{I}}s_{\text{Q}}} = 2|H_u(k)|^2\left[S_{\text{I}}^{\text{r}}(k)S_{\text{Q}}^{\text{r}}(k) + S_{\text{I}}^{\text{i}}(k)S_{\text{Q}}^{\text{i}}(k)\right]/M$ and $F_{sw} = 2[(H_u(k)S(k))^{\text{r}}\, W^{\text{r}}(k) + (H_u(k)S(k))^{\text{i}}\, W^{\text{i}}(k)]/M = F_{sw}^{\text{e}} + F_{sw}^{\text{o}}$ are cross-PSDs, with $F_{s_{\text{I}}s_{\text{Q}}}$ being circular-odd.

Denoting $\mathbb{E}[\cdot]$ as the expectation operation, it follows that $\mathbb{E}[F'_u(k)] = \mathbb{E}[F_{s_{\text{I}}}] + \mathbb{E}[F_{s_{\text{Q}}}] + \mathbb{E}[F_w^{\text{e}}]$, since $\mathbb{E}[F_w^{\text{o}}] = 0$ from the definition of the odd component of a sequence and the independence between different elements of $W(k)$, and $\mathbb{E}[F_{sw}^{\text{e}}] = \mathbb{E}[F_{sw}^{\text{o}}] = 0$ from the independence between signal and noise. Consequently, $\mathbb{E}[F'_u(k)] = \mathbb{E}[F_u(k)]$, meaning that the circular-even operation given by (1) does not change the mean of $F'_u(k)$ with respect to $F_u(k)$.

To compute the variance of $F'_u(k)$ and $F_u(k)$, the pairwise covariances of the right-hand side terms of (2) and (3) must be derived. From [1, eqs. (11) and (12)], $\mathbb{E}[W(k)] = \mathbb{E}[W^{\text{r}}] = \mathbb{E}[W^{\text{i}}] = 0$, and from the assumption of zero-mean $s_{\text{I}}(n)$ and $s_{\text{Q}}(n)$, $\mathbb{E}[S(k)] = \mathbb{E}[S_{\text{I}}^{\text{r}}(k)] = \mathbb{E}[S_{\text{I}}^{\text{i}}(k)] = \mathbb{E}[S_{\text{Q}}^{\text{r}}(k)] = \mathbb{E}[S_{\text{Q}}^{\text{i}}(k)] = 0$. Stemming from the fact that the covariance $\mathbb{C}[\cdot,\cdot]$ between the random variables X and Y is $\mathbb{C}[Z,Y] = \mathbb{E}[ZY] - \mathbb{E}[Z]\mathbb{E}[Y]$, and from the definition of the circular-even and circular-odd components of a sequence, one can prove that $2\mathbb{C}[F_{s_{\text{I}}}, F_{s_{\text{I}}s_{\text{Q}}}] = 2\mathbb{C}[F_{s_{\text{Q}}}, F_{s_{\text{I}}s_{\text{Q}}}] = 2\mathbb{C}[F_{s_{\text{I}}}, F_w^{\text{e}}] = 2\mathbb{C}[F_{s_{\text{I}}}, F_w^{\text{o}}] = 2\mathbb{C}[F_{s_{\text{Q}}}, F_w^{\text{e}}] = 2\mathbb{C}[F_{s_{\text{Q}}}, F_w^{\text{o}}] = 2\mathbb{C}[F_{s_{\text{I}}s_{\text{Q}}}, F_w^{\text{e}}] = 2\mathbb{C}[F_{s_{\text{I}}s_{\text{Q}}}, F_w^{\text{o}}] = 2\mathbb{C}[F_{s_{\text{I}}}, F_{sw}^{\text{e}}] = 2\mathbb{C}[F_{s_{\text{I}}}, F_{sw}^{\text{o}}] = 2\mathbb{C}[F_{s_{\text{Q}}}, F_{sw}^{\text{e}}] = 2\mathbb{C}[F_{s_{\text{Q}}}, F_{sw}^{\text{o}}] = 2\mathbb{C}[F_{s_{\text{I}}s_{\text{Q}}}, F_{sw}^{\text{e}}] = 2\mathbb{C}[F_w^{\text{e}}, F_{sw}^{\text{e}}] = 2\mathbb{C}[F_w^{\text{o}}, F_{sw}^{\text{e}}] = 2\mathbb{C}[F_{sw}^{\text{e}}, F_{sw}^{\text{o}}] = 2\mathbb{C}[F_w^{\text{e}}, F_{sw}^{\text{o}}] = 2\mathbb{C}[F_w^{\text{o}}, F_{sw}^{\text{o}}] = 2\mathbb{C}[F_{s_{\text{I}}s_{\text{Q}}}, F_{sw}^{\text{o}}] = 2\mathbb{C}[F_w^{\text{e}}, F_w^{\text{o}}] = 0$.

The variance of $F'_u(k)$ is then $\mathbb{V}[F'_u(k)] = \mathbb{V}[F_{s_{\text{I}}}] + \mathbb{V}[F_{s_{\text{Q}}}] + \mathbb{V}[F_{s_{\text{I}}s_{\text{Q}}}] + \mathbb{V}[F_w^{\text{e}}] + \mathbb{V}[F_w^{\text{o}}] + \mathbb{V}[F_{sw}^{\text{e}}] + \mathbb{V}[F_{sw}^{\text{o}}] + 2\mathbb{C}[F_{s_{\text{I}}}, F_{s_{\text{Q}}}]$. Analogously, the variance of $F_u(k)$ is $\mathbb{V}[F_u(k)] = \mathbb{V}[F_{s_{\text{I}}}] + \mathbb{V}[F_{s_{\text{Q}}}] + \mathbb{V}[F_w^{\text{e}}] + \mathbb{V}[F_{sw}^{\text{e}}] + 2\mathbb{C}[F_{s_{\text{I}}}, F_{s_{\text{Q}}}]$, yielding $\mathbb{V}[F_u(k)] = \mathbb{V}[F'_u(k)] - \mathbb{V}[F_{s_{\text{I}}s_{\text{Q}}}] - \mathbb{V}[F_w^{\text{o}}] - \mathbb{V}[F_{sw}^{\text{o}}]$, from where it is straightforward to conclude that $\mathbb{V}[F_u(k)] < \mathbb{V}[F'_u(k)]$. This inequality means that the variance of the decision variables $r_{\text{avg}}(\ell)$ in the proposed CF-CPSC will be smaller than the ones of the original CPSC, since they are formed from $F_u(k)$. Recalling that the mean of $F'_u(k)$ and $F_u(k)$ are the same for $k > 1$, this will lead to an improvement in the CF-CPSC performance with respect to the CPSC.

III. Analytical Results under $\mathcal{H}_0$

A. Cumulative Distribution Functions

Under $\mathcal{H}_0$, the DFT of the received signal is $X_u(k) = W_u(k)$. Then, $F'_u(k)$ can be written as $F'_u(k) = [W_u^{\text{r}}(k)/\sqrt{M}]^2 + [W_u^{\text{i}}(k)/\sqrt{M}]^2$. With this result in (1), $F_u(k)$ can be expressed as in (4) (at the top of the next page).

It is shown in [1, eqs. (13) and (17)] that $W_u^{\text{r}}(k)$ and $W_u^{\text{i}}(k)$ are zero-mean uncorrelated Gaussian random variables with variance $M\sigma_u^2/2$. Therefore $W_u^{\text{r}}(k)/\sqrt{M}$ and $W_u^{\text{i}}(k)/\sqrt{M}$ are Gaussian random variables with zero mean and variance $\sigma_u^2/2$. Knowing that $W_u(k)$ is uncorrelated of $W_u(j)$ for $k \neq j$ [1, eq. (21)], and applying (4) in $F_{\ell,u}$ and F_{full_u}, one can verify that the numerator and the denominator of $r_u(\ell)$ are Gamma distributed, as they are composed by the sum of squared, zero-mean, equal variance Gaussian random variables. Notice that the modification in the circular-even operation described in step ② was made to guarantee that $F_u(1)$ has the same distribution of $F_u(k)$ for $k = 2, 3, \ldots, M/2$ under $\mathcal{H}_0$.

Let Z_1 and Z_2 be independent Gamma random variables with respective scale and shape parameters (b, c_1) and (b, c_2). The random variable $Y = Z_1/(Z_1 + Z_2)$ will follow a Beta distribution with shape parameters c_1 and c_2 [4, Chapter 8]. Since the denominator of $r_u(\ell)$ can be split into the sum of two Gamma random variables with shape parameters $c_1 = 2V$ and $c_2 = M - 2V$, then $r_u(\ell)$ follows a Beta distribution with parameters $c_1 = 2V$ and $c_2 = M - 2V$. Therefore, the closed-form conditional CDF of $r_u(\ell)$, that is $F_{r_u(\ell)}(r) = \Pr[r_u(\ell) < r|\mathcal{H}_0]$, is given by

$$F_{r_u(\ell)}(r) = I_r\left(2V, M - 2V\right), \tag{5}$$

$$F_u(k) = \begin{cases} [W_u^{\mathrm{r}}(k)^2 + W_u^{\mathrm{i}}(k)^2 + W_u^{\mathrm{r}}(M/2+1)^2 + W_u^{\mathrm{i}}(M/2+1)^2]/(2M), & k = 1. \\ [W_u^{\mathrm{r}}(k)^2 + W_u^{\mathrm{i}}(k)^2 + W_u^{\mathrm{r}}(M-k+2)^2 + W_u^{\mathrm{i}}(M-k+2)^2]/(2M), & k = 2, 3, \ldots, M. \end{cases} \quad (4)$$

where $I_r(\cdot,\cdot)$ is the incomplete regularized Beta function [5, (8.392)], which is a built-in function in many mathematical software packages such as Matlab and Mathematica.

In the case of $r_{\text{avg}}(\ell)$, it is distributed as the sum of Beta random variables, which has not a general solution. The authors of [1], under another assumption for the underlining distributions, considered that of $r_{\text{avg}}(\ell)$ has approximately the same distribution of $\sum_{u=1}^{U} F_{\ell,u} / \sum_{u=1}^{U} F_{\text{full}_u}$. Applying this reasoning to our analysis, it follows that $\sum_{u=1}^{U} F_{\ell,u} / \sum_{u=1}^{U} F_{\text{full}_u}$ will be the quotient between the sum of Gamma random variates, yielding a Beta random variate. Then, $r_{\text{avg}}(\ell)$ will follow a Beta distribution with parameters $c_1 = 2VU$ and $c_2 = (M - 2V)U$, for which the closed-form conditional CDF, $F_{r_{\text{avg}}(\ell)}(r) = \Pr[r_{\text{avg}}(\ell) < r|\mathcal{H}_0]$, is

$$F_{r_{\text{avg}}(\ell)}(r) = I_r\left(2VU, (M-2V)U\right). \quad (6)$$

B. Probability of False Alarm

Consider the random vector $\mathbf{R} = [R_1, R_2, \ldots, R_L]^{\mathrm{T}}$ with elements $R_\ell \triangleq r_{\text{avg}}(\ell)$, $\ell = 1, 2, \ldots, L$, where $[\cdot]^{\mathrm{T}}$ means transpose. Since each element of $\mathbf{R}$ is a Beta random variable, the joint PDF (JPDF) $f_{\mathbf{R}}(r_1, r_2, \ldots, r_{L-1})$ will follow a Dirichlet distribution [6], which is the multivariate generalization of the Beta distribution [4, Chapter 13], that is,

$$f_{\mathbf{R}}(r_1, r_2, \ldots, r_{L-1}) = \frac{\Gamma(2VUL)}{\Gamma(2VU)^L} \prod_{\ell=1}^{L-1} (r_\ell r_L)^{2VU-1}, \quad (7)$$

with $r_L = 1 - \sum_{i=1}^{L-1} r_i$, $r_\ell \geq 0$ for all ℓ, and $\sum_{\ell=1}^{L-1} r_\ell \leq 1$.

The joint CDF (JCDF) of $\mathbf{R}$ is $F_{\mathbf{R}}(\mathbf{r}) \triangleq F_{\mathbf{R}}(r_1, r_2, \ldots, r_L)$, with $r_1, r_2, \ldots, r_L$ corresponding to the threshold γ, i.e. $r_\ell = \gamma$. From step ⑦ of the CF-CPSC algorithm, one can see that $F_{\mathbf{R}}(\mathbf{r})$ is the probability that the FC decides in favor of $\mathcal{H}_0$. Thus, the global PFA can be computed as

$$P_{\text{fa}}(\gamma) = 1 - F_{\mathbf{R}}(\gamma), \quad (8)$$

where the JCDF of $\mathbf{R}$ is given by

$$F_{\mathbf{R}}(\gamma) = \int_0^\gamma \cdots \int_0^\gamma f_{\mathbf{R}}(r_1, \ldots, r_{L-1}) \mathrm{H}(\gamma - r_L)\, dr_1 \cdots dr_{L-1},$$

and where $\mathrm{H}(\cdot)$ is the Heaviside step function [5]. Notice that $f_{\mathbf{R}}(r_1, r_2, \ldots, r_{L-1})$ is not an explicit function of r_L, since r_L is expressed as a function of the other variables r_i, $i < L$. Then, if equation (7) is directly integrated, the domain constraint defined by $r_L < \gamma$ would not be satisfied. The multiplication of (7) by $\mathrm{H}[\gamma - (1 - \sum_{i=1}^{L-1} r_i)]$ will be (7) itself if $1 - \sum_{i=1}^{L-1} r_i < \gamma$, and zero otherwise, which accounts for $r_L < \gamma$ as needed.

C. A Simple Closed-Form Probability of False Alarm

If it is considered that the decisions at the sub-band level are approximately independent of each other, which means independence among the elements of $\mathbf{R}$, (8) simplifies to

$$\tilde{P}_{\text{fa}}(\gamma) = 1 - \{I_\gamma\left(2VU, (M-2V)U\right)\}^L. \quad (9)$$

It was found in [2, eq. (17)] that any two elements R_i and R_j of $\mathbf{R}$, for $i \neq j$, exhibit a correlation coefficient $\rho_{R_i R_j} = -1/(L-1)$, from where one can promptly infer that $\rho_{R_i R_j} \to 0$ as the number of sub-bands increases. Then, for sufficiently large values of L, (9) becomes valid since $F_{\mathbf{R}}(r, r, \ldots, r|\mathcal{H}_0)$ can be written as the CDF of R_ℓ raised to the L-th power. We postpone the discussion about the accuracy and usefulness of this approximation to the next section.

The decision threshold for a target PFA P_{faT} can be determined from (9) using the inverse incomplete regularized Beta function, which is also present in many mathematical softwares. Specifically, $\gamma = I^{-1}_{(1-P_{\text{faT}})^{1/L}}\left(2VU, (M-2V)U\right)$.

IV. Numerical Results and Discussion

In this section, the performances of the CF-CPSC and the original CPSC are compared. The eigenvalue-based generalized likelihood ratio test (GLRT) is also considered, since it is one of the best-performing detectors under the unknown noise level condition [7]; the GLRT statistic is the ratio between the maximum eigenvalue and the average eigenvalues of the received signal covariance matrix. Subsequently, the empirical PFA is contrasted with the PFA obtained from (8) and (9). The PU transmits a quaternary phase-shift keying (QPSK) signal at baseband level with 4 samples per symbol; other modulation could be adopted as well. The sensing interval corresponds to 40 symbols, yielding $M = 160$ samples collected by each CR. The number of sub-bands is $L = 5$. The shadowed-fading channel tap gains in $h_u(z)$ follow a log-normal shadowing combined with a Rayleigh fading. The gains are fixed during each sensing interval, and independent between successive intervals, different CRs and different taps. The shadowing process has a standard deviation of 4 dB, is independent between different sensing intervals, and is correlated between different CRs; the correlation level was established from a practical decorrelation distance [8] of 30 meters. When the PU-SU channel is flat, we let $Z = 1$; otherwise $Z = 4$ to represent a highly frequency-selective fading, since the delay spread in this case is equal to the symbol length. The impulse response follows a typical outdoor negative exponential shape, with average tap gains $[1, 0.464, 0.215, 0.1]$. The signal-to-noise ratio (SNR) is -10 dB to represent a low SNR regime. When the noise variances at the input of the CRs are unequal, which is a common situation in practice, they are $[0.8, 0.9, 0.95, 1.1, 0.85, 1.15]$; otherwise they are unitary. Each value of the empirical PFA and probability of detection (PD) was computed from 50000 Monte Carlo events.

Fig. 1 shows receiver operating characteristic (ROC) curves considering frequency-flat fading PU-SUs channels, with equal noise variances and no shadowing. It can be seen that the CF-CPSC expressively outperforms the CPSC in all cases. The GLRT wins due to the favorable and not realistic equal noise variance condition. It can also be noticed the expected

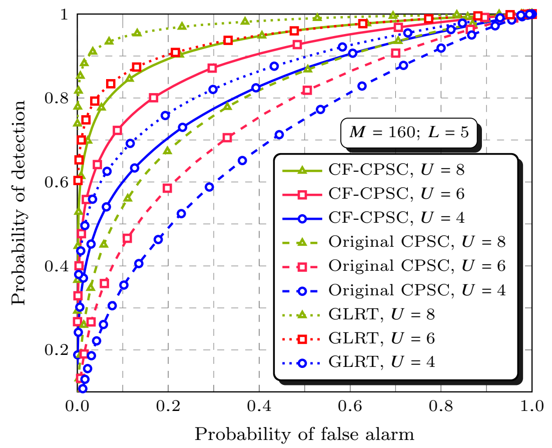

Fig. 1. ROC curves considering frequency-flat PU-SUs fading channels, equal noise variances and no shadowing.

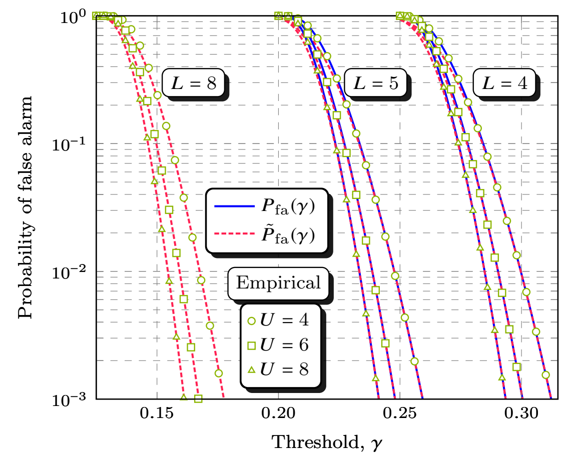

Fig. 2. Global PFA using (8), (9), and simulation (symbols) with $M = 160$.

TABLE I
AREAS UNDER ROC CURVES

PU-SU channel Scenario	CF-CPSC	CPSC	GLRT
1. flat, no shadowing, equal noise	0.8935	0.7615	**0.9385**
2. selective, no shadowing, equal noise	0.8921	0.7655	**0.9234**
3. selective, shadowing, equal noise	**0.8504**	0.7355	0.8240
4. selective, shadowing, unequal noise	**0.8631**	0.7504	0.6037

performance improvement as the number U of CRs increases, which is due to the diversity gain achieved with CSS.

Table I lists the areas under the ROC curves (AUC) for the detection techniques under analysis, considering scenarios of frequency-flat or -selective fading PU-SUs channels, with presence or absence of spatially-correlated shadowing, and equal or unequal noise variances at the CRs' inputs. The same system parameters considered in Fig. 1 were adopted, but only for $U = 6$ SUs. The AUCs for Scenario 1 correspond to Fig. 1, $U = 6$. The presence of frequency selectivity in Scenario 2 slightly degrades the performance of all detectors. Keeping in mind that the signal is distorted but its power is not changed on average, this is an expected result. The presence of shadowing in Scenario 3 is responsible for a noticeable performance degradation of all detectors, especially of the GLRT. In this more realistic scenario, the CF-CPSC outperforms the CPSC and the GLRT. The most realistic Scenario 4 considers the presence of frequency selectivity, shadowing and unequal noise variances. In this case the performances of the CF-CPSC and the CPSC remain practically unchanged with respect to Scenario 3, which is due to the intrinsic robustness of these techniques to dynamical noise. The GLRT, however, suffers from a drastic performance penalty in this scenario. Finally, from Table I it can be concluded that both the CF-CPSC and the CPSC are able to maintain their performances practically unchanged under the variation in the channel scenario, with the CF-CPSC always winning.

Fig. 2 contrasts $P_{\text{fa}}(\gamma)$, as given by (8), the approximate $\tilde{P}_{\text{fa}}(\gamma)$, as given by (9), and empirical (symbols) PFAs obtained from simulations under the $\mathcal{H}_0$ hypothesis. Besides the parameters considered to plot Fig. 1, results for $L = 4$ and $L = 8$ sub-bands were added. From this figure one can see that all empirical PFA curves are in very close agreement with the theoretical ones, especially for PFA below 0.2, which is a typical operation region of the spectrum sensing system. As the number of sub-bands L is increased, it is noteworthy that whereas (8) might take hours and prompt lots of warning while computed in Mathematica (or even not handled, when $L = 8$ for instance), the approximate formula (9) is computed practically instantaneously in Mathematica and Matlab, independently of the number of sub-bands. Nevertheless, it is indeed when L becomes large that the correlation coefficient $\rho_{R_i R_j}$ becomes small, favoring the use of (9) instead of (8).

In summary, in this letter we have proposed a new CF-CPSC algorithm and made a theoretical analysis of its performance in terms of PFA. The numerical results validated the theoretical achievements and unveiled expressive improvements of the CF-CPSC over the original CPSC, which stems from the noise variance reduction in the decision variables of the proposed CF-CPSC with respect to the original CPSC (see II-B). The numerical results also demonstrated the superiority of the CF-CPSC over the GLRT in the practical appealing scenarios of frequency-selective shadowed-fading channels with different noise levels at the CRs.

REFERENCES

[1] R. Gao, Z. Li, P. Qi, and H. Li, "A robust cooperative spectrum sensing method in cognitive radio networks," *IEEE Commun. Lett.*, vol. 18, no. 11, pp. 1987–1990, Nov. 2014.

[2] R. C. D. V. Bomfin, D. A. Guimarães, and R. A. A. de Souza, "On the probability of false alarm of the power spectral density split cancellation method," *IEEE Wireless Commun. Lett.*, vol. 5, no. 2, pp. 164–167, Apr. 2016.

[3] V. K. Ingle and J. G. Proakis, *Digital Signal Processing Using MATLAB*, 3rd ed. Pacific Grove, CA, USA: Brooks/Cole Publishing Co., 2012.

[4] C. Forbes, M. Evans, N. Hastings, and B. Peacock, *Statistical Distributions*, 4th ed. Wiley, 2011.

[5] A. Jeffrey, D. Zwillinger, I. Gradshteyn, and I. Ryzhik, *Table of Integrals, Series, and Products*, 7th ed. Wiley, 2007.

[6] B. A. Frigyik, A. Kapila, and M. R. Gupta, "Introduction to the Dirichlet distribution and related processes," *UWEE Technical Report Series*, 2010.

[7] B. Nadler, F. Penna, and R. Garello, "Performance of eigenvalue-based signal detectors with known and unknown noise level," in *2011 IEEE International Conference on Communications (ICC)*, Jun. 2011, pp. 1–5.

[8] R. C. D. V. Bomfin and R. A. A. de Souza, "A new spatially correlated shadowed channel model with cognitive radio application," in *2015 IEEE 81st Veh. Tech. Conf. (VTC Spring)*, May 2015, pp. 1–5.